J Mater Sci: Mater Med (2009) 20:1229–1236
DOI 10.1007/s10856-009-3690-8

Preparation of porous 45S5 Bioglass®-derived glass–ceramic scaffolds by using rice husk as a porogen additive

Shih-Ching Wu · Hsueh-Chuan Hsu · Sheng-Hung Hsiao · Wen-Fu Ho

Received: 9 August 2008 / Accepted: 6 January 2009 / Published online: 22 January 2009

Abstract Bioactive glass is currently regarded as the most biocompatible material in the bone regeneration field because of its bioactivity, osteoconductivity and even osteoinductivity. In the present work porous glass–ceramic scaffolds, which were prepared from the 45S5 Bioglass® by foaming with rice husks and sintering at 1050°C for 1 h, have been developed. The produced scaffolds were characterized for their morphology, properties and bioactivity. Micrographs taken using a scanning electron microscope (SEM) were used for analysis of macropores, mesopores and micropores, respectively. The bioactivity of the porous glass–ceramic scaffolds was investigated using simulated body fluid (SBF) and characterized by SEM, energy dispersive spectroscopy (EDS) and X-ray diffraction (XRD). A great potential scaffold that provides sufficient mechanical support temporarily while maintaining bioactivity, and that can biodegrade at later stages is achievable with the developed 45S5 Bioglass®-derived scaffolds.

S.-C. Wu · H.-C. Hsu
Department of Dental Laboratory Technology, Central Taiwan University of Science and Technology, Taichung, Taiwan, ROC

S.-C. Wu · H.-C. Hsu
Institute of Biomedical Engineering and Material Science, Central Taiwan University of Science and Technology, Taichung, Taiwan, ROC

S.-H. Hsiao
Department of Mechanical and Automation Engineering, Da-Yeh University, Dacun, Changhua, Taiwan, ROC

W.-F. Ho (✉)
Department of Materials Science and Engineering, Da-Yeh University, No. 112, Shanjiao Rd, Dacun, Changhua 51591, Taiwan, ROC
e-mail: fujii@mail.dyu.edu.tw

1 Introduction

Bone tissue engineering, involving the fabrication of a porous scaffold, has become an alternative approach to promote the repair and regeneration of diseased or damaged bone tissue [1]. The specific criteria for ideal scaffolds used in bone tissue engineering includes ability to deliver cells, excellent osteoconductivity, good biodegradability, appropriate mechanical properties, pore sizes at least 100 μm, irregular shape fabrication ability and commercialization potential [2–4]. Porosity is the relevant feature these scaffolds must fulfill. The ideal structures must be formed by an interconnected porous network with a wide variety of pore sizes, large pores that allow tissue ingrowth and vascularization of the new formed tissue, and pores in the microporous range to promote protein adhesion and consequently cell adhesion and proliferation. It has been recognized that the pore structure is one of the decisive factors affecting the biological function of scaffolds [5, 6]. To imitate the porous structure of spongy bone, many techniques have been developed, such as polymeric sponge replication [7], gel-casting techniques [8], freeze drying [9], particulate leaching [10], solvent casting [11] and rapid prototyping techniques [12]. These techniques endow scaffolds with a variety of porous microstructures to satisfy different applications.

Bioactive glasses possess excellent osteoconductivity, bioactivity [13–17], ability to deliver cells [18], and controllable biodegradability [19–21]. These advantages make bioactive glasses promising scaffold materials for tissue engineering [22, 23]. The ability of bioactive glasses and glass–ceramics to bond to bone in vivo through the formation of a hydroxyapatite surface layer is well-documented [15, 24, 25]. Recently, 45S5 Bioglass® based porous scaffolds have been promoted for tissue engineering

strategies [26–28]. Bioglass® is nowadays used successfully as middle ear and dental implants [29].

Rice husk is an abundantly available waste material in all rice producing countries. Rice husk consists of organic materials (e.g. cellulose, hemicellulose and lignin) (~75 wt%), amorphous SiO_2 (~15 wt%) and water (~10 wt%) [30]. In certain regions, it is sometimes used as a fuel for parboiling paddy in the rice mills. The partially burnt rice husk in turn contributes to more environmental pollution. There have been efforts not only to overcome this but also to find value addition to these wastes using them as secondary source of materials [31]. Keeping this view in mind, in respect of environmental friendly and cost-effectiveness, the rice husk powders were used as an additive to produce porous structure of 45S5 Bioglass® scaffolds.

The objectives of this work were to synthesize 45S5 Bioglass® scaffolds using the porogen burnout technique, to achieve mechanically stable scaffolds through a tailored sintering schedule, and to assess the bioactivity and biodegradability of the scaffolds. To the best of our knowledge, there is no report on the preparation of 45S5 Bioglass® scaffolds from rice husk additives. In this study, the 45S5 Bioglass® was used as the base material. Organic additives, rice husks, were employed to produce structures with large and small pores for the first time. The final goal is to create an ideal scaffold for bone tissue engineering application.

2 Materials and methods

2.1 Materials

For the elaboration of the porous scaffolds, 45S5 Bioglass® was used as the base material. 45S5 Bioglass® (45.0 SiO_2, 24.5 CaO, 24.5 Na_2O, 6.0 P_2O_5 in wt%) was obtained from high-purity SiO_2, Na_2CO_3, $CaCO_3$ and P_2O_5 powders. The powders were weighed, mixed and melted in a Pt crucible for 1.5 h at 1400°C. The produced glass was quenched in cold water and then crushed in an agate mortar. It was then planetary ball milled in ethanol. The glass particles were dried in an oven at 100°C overnight, then disaggregated in an agate mortar and sieved. The glass particles were sieved through a #200 and #500 mesh to obtain particles with a size less than 25 μm and 25–75 μm. The rice husks (Taigeng 8, variety) with an average particle size of about ≤355 μm and 355–600 μm were used as pore formers, respectively. The rice husks contain anisotropic plate-like particles because of their shell structure.

2.2 Scaffold fabrication

45S5 Bioglass® powders were mixed with different percentages of rice husks. An aqueous solution of PVA with a concentration of 0.1 mol/l was prepared. Once mixed homogeneously, the mixture was used to produce green bodies by uniaxial pressing at 100 kg/cm^2. The pressed samples were heat treated to burn out the rice husk additives and binder (PVA) at 450°C for 1 h at a heating rate of 1°C/min and then sintered at 1050°C for 1 h at a heating rate of 5°C/min. The specimen codes are shown in Table 1.

2.3 Characterization of the scaffolds

Apparent density was calculated for each specimen, which was calculated from the dry weight and volume of each sintered specimen. The porosity P was then calculated by

$$\text{Porosity} = 1 - (\text{Apparent density}/\rho_{\text{Glass}}) \quad (1)$$

where $\rho_{\text{Glass}} = 2.7$ g/cm^3 is the density of solid 45S5 Bioglass® [21].

Micrographs taken using a scanning electron microscope (SEM; JSM-6700F, JEOL, Japan) were used for analysis of macrostructure and microporosity, respectively. Macropore lengths and breadths were measured, where the macropore length is the dimension of the longest axis, and macropore breadth the longest dimension perpendicular to the length.

2.4 Compressive testing

The compressive strength was measured using a desk-top mechanical tester (AG-IS, Shimadzu, Japan) at a crosshead speed of 0.5 mm/min. The samples were rectangular in shape, with dimensions: 5 mm in height and 10 mm × 10 mm in cross-section. At least five samples were tested for each condition and the results were averaged. During the compression test, the load was applied until densification of the porous samples started to occur. The compression

Table 1 Specimen codes according to the 45S5 Bioglasss® and rice husk content and particle size

Material code	45S5 Bioglasss® (wt%)	Rice husk (wt%)	45S5 Bioglasss® particle size (μm)	Rice husk particle size (μm)
20GL80RS	20	80	25–75	≤355
30GL70RL	30	70	25–75	355–600
25GS75RL	25	75	≤25	355–600

mechanical test follows the guidelines set in ASTM D5024-95a.

2.5 Assessment of bioactivity in simulated body fluid

The in vitro degradability of the macroporous scaffolds was evaluated in simulated body fluid (SBF). The temperature was maintained by using a water bath. The SBF was prepared by dissolving reagent grade NaCl, $NaHCO_3$, KCl, $K_2HPO_4 \cdot 3H_2O$, $MgCl_2 \cdot 6H_2O$, $CaCl_2$, and Na_2SO_4 into distilled water. The final ionic concentrations of the SBF (versus human plasma) are listed in Table 2 [32]. The SBF was refreshed every 2 days to preserve its ion concentration. After being immersed for selected time periods (3, 7, 14 and 28 days), the specimens were removed from the fluid, rinsed gently with distilled water and left to dry at ambient temperature in a desiccator. After being soaked for 28 days, the compressive strengths of the scaffolds were measured. SEM on gold-coated specimens was used to examine the microstructure of the scaffolds before and after immersion in SBF. Selected scaffolds were also characterized using X-ray diffraction (XRD; XRD-6000, Shimadzu, Japan) analysis with the aim to assess the crystallinity after sintering and formation of apatite on surfaces after different times of immersion in SBF. The scaffolds were first ground into a powder. Then 0.5 g of the powder was collected for XRD analysis operated at 30 kV and 30 mA, from 2θ values of 20° to 60°.

3 Results and discussion

3.1 Crystallization of 45S5 Bioglass® powders

In order to evaluate qualitatively the level of devitrification or formation of crystalline phases in the material, XRD analysis was performed. Figure 1 shows XRD spectra for 45S5 Bioglass® powder unsintered and sintered at 450, 650, 850 and 1050°C for 1 h. Spectra of 45S5 Bioglass® sintered at 450°C showed that the powders were amorphous. However the spectra of 45S5 Bioglass® sintered at 650°C or higher exhibited peaks that were indicative of apatite and crystalline phase $Na_2Ca_2Si_3O_9$. The XRD investigation revealed that crystallization had occurred extensively in all samples sintered at higher 650°C for 1 h. Moreover, the 45S5 Bioglass® powders heat-treated at 1050°C showed very sharp X-ray powder lines. $Na_2Ca_2Si_3O_9$, identified as the major phase present, was also identified in previous studies of bioactive 45S5 Bioglass® crystallization [33–36]. This is as indicated in the finding of Clupper and Hench [37] that extensive crystallization occurs prior to significant viscous flow sintering in 45S5 Bioglass® and related bioactive glasses. Moreover, Chen et al. [36] reported that the bonding of 45S5 Bioglass® particles was not obvious at the sintering condition of 900°C for 5 h. The combination of extensive densification and the presence of a crystalline phase in the scaffolds sintered at 1050°C for 1 h are expected to lead to improved mechanical properties of these specimens. Hence microstructure, mechanical tests and assessment of bioactivity in SBF were carried out on scaffolds sintered at 1050°C for 1 h.

3.2 Porous structure of scaffolds

Figure 2a–c shows the morphology of the fracture surface of specimens with three different conditions after sintering at 1050°C for 1 h. All these samples show a structure mainly formed by elongated pores. The shapes and sizes of the pores are similar to those of the rice husks. SEM demonstrated that porosity could be classified into two groups, divisible by size. Macropores (>420 μm in length and >100 μm in breadth) elongated in shape and oriented. Mesopores (25–80 μm in size) tended to be isolated spherical pores, which were randomly distributed throughout the specimens.

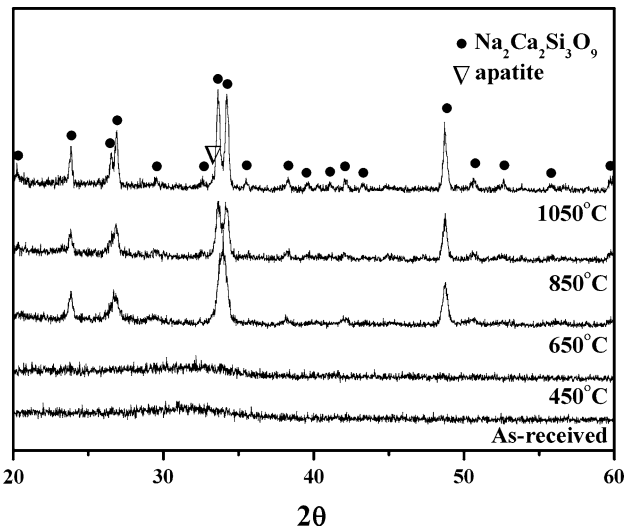

Fig. 1 XRD spectra for 45S5 Bioglass® powder unsintered and sintered at 450, 650, 850 and 1050°C for 1 h

Table 2 Ionic concentrations (mM) of SBF compared to human blood plasma

	Na^+	K^+	Mg^{2+}	Ca^{2+}	Cl^-	HPO_4^{2-}	SO_4^{2-}	HCO_3^-
SBF	142.0	5.0	1.5	2.5	148.8	1.0	0.5	4.2
Blood plasma	142.0	5.0	1.5	2.5	103.8	1.0	0.5	27.0

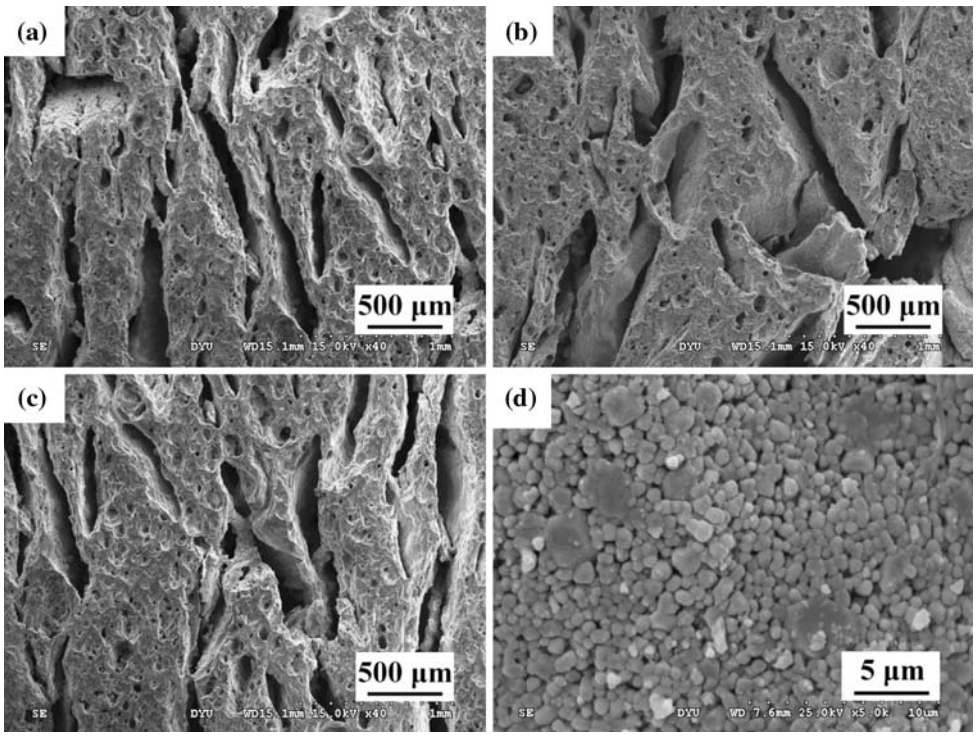

Fig. 2 SEM micrographs of **a** 20GL80RS, **b** 30GL70RL and **c** 25GS75RL scaffolds sintered at 1050°C for 1 h. **d** Macropore surface of scaffolds under higher magnification

The picture under higher magnification showed that the macropore surface of scaffolds was very rough and many micropores existed (Fig. 2d). As shown in Fig. 3, the <2 µm micropores, which were formed during the sintering process as a result of grain growth and coalescence, were located on triple points and within grains and as such would be expected to be isolated from both each other and the external surfaces. The micropores in the macropore surface enlarged greatly the surface area for protein adsorption. Therefore, more proteins could be absorbed on the surface. The larger surface area could also facilitate ion exchanges and bone-like apatite surface formation by the dissolution and re-precipitation process [38]. More proteins absorbed on the pore surfaces and the easier formed apatite layer may facilitate bone formation [39]. The micropores could also provide a suitable microenvironment for cell differentiation and bone matrix deposition [40].

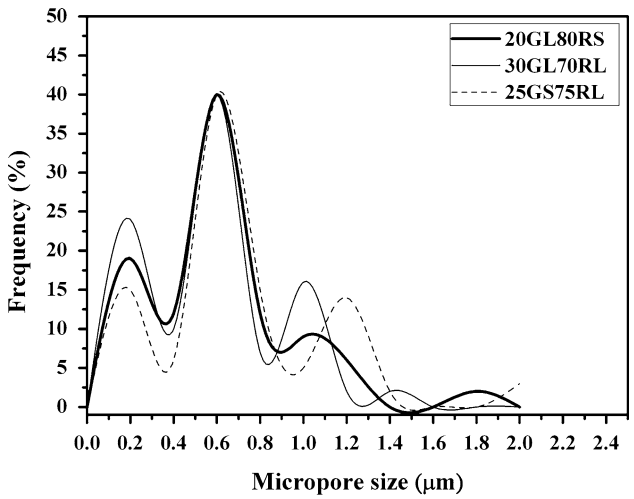

Fig. 3 Micropore size distribution of scaffolds

3.3 Compressive strength

Conventional methods of mechanical characterization such as tensile, biaxial and impact testing are unsuitable when applied to porous materials due to the difficulties encountered in machining and gripping test pieces without causing pre-damage [41]. Compression testing has been successfully used by a number of authors in the characterization of cancellous bone and has also been adopted in the testing of porous biomaterials [36, 42, 43]. Compressive strength tests were carried out on specimens sintered at 1050°C for 1 h and after immersion in SBF for 28 days. Figure 4 shows a stress-strain curve typical of the behavior of scaffolds undergoing compressive testing in this study. The three regimes of stress-strain curve are the typical behavior of scaffolds under compression [36, 44]. Figure 4 shows also that the scaffolds failed as typical porous brittle materials [44]. The specimens tend to crack first at stress-concentrating sites, causing the apparent stress to drop temporarily. But the specimens, as a whole, still had the ability to bear higher loads, causing the stress to rise again. The repetition of this procedure gave a jagged stress-strain curve.

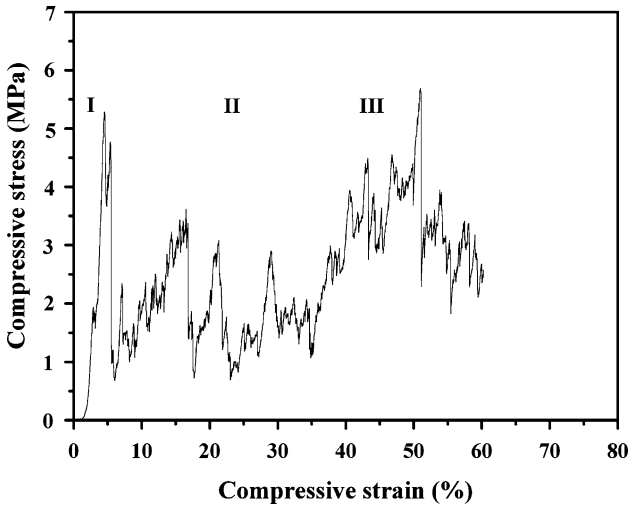

Fig. 4 A typical compressive stress-strain curve of the 45S5 Bioglass®-derived scaffolds

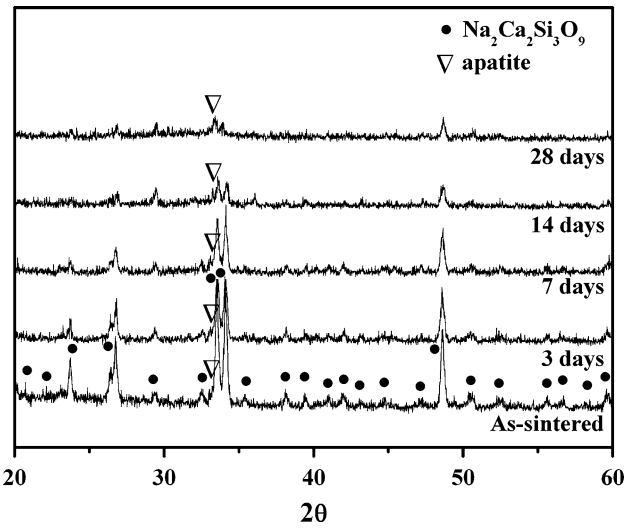

Fig. 5 XRD spectra of 45S5 Bioglass®-derived scaffolds sintered 1050°C for 1 h, and following 3, 7, 14 and 28 days SBF immersion

In general, the compressive strength of the scaffolds decreased as the porosity increased [38]. Unexpectedly, the 20GL80RS scaffolds exhibited much higher mechanical properties than the 30GL70RL and 25GS75RL counterparts (Table 3), although the porosity is higher than 25GS75RL and lower than 30GL70RL. This result could be related to the small macropore size of 20GL80RS using smaller rice husk size (Fig. 3a). On the other hand, the compressive strength is only 5.4 MPa for the 25GS75RL scaffolds with much higher porosity and lower apparent density. The compressive tests were frequently accompanied by shearing, which was mainly caused by the end effects imposed on the specimen during the test. It has been reported that if the faces of the porous specimen are slightly misaligned with the loading platen, large stress concentrations can occur causing local buckling, which in turn leads to shearing and thus results in an underestimation of the strength [45]. As a result, the compressive strengths of scaffolds had large variations in the present work. ANOVA test results showed that there are no significant differences among the compressive strengths of 20GL80RS, 30GL70RL and 25GS75RL scaffolds ($P > 0.05$).

In addition, it has been reported that the compressive strength of a hydroxyapatite scaffold significantly increases (e.g. from ~10–30 MPa [46]) due to tissue ingrowth in vivo. It has also been speculated that it might not be necessary to fabricate a scaffold with a mechanical strength equal to bone because cultured cells on the scaffold and new tissue formation in vitro will create a biocomposite and will increase the time-dependent strength of the scaffold significantly [22]. An ideal scaffold, however, should have at least a proper strength to allow it to be manipulated adequately for tissue engineering applications. In the present work, compressive strengths were achieved in the ranges of 5.4–7.2 MPa, which is within the compressive strength (between 2 and 12 MPa) of trabecular bone [47]. In addition, Chen et al. [36] indicated that the strength of 0.3–0.4 MPa is sufficient for the foam to be handled with, such as manipulating during SBF tests and cutting of the samples for mechanical tests. The present 45S5 Bioglass®-derived scaffolds possess such an appropriate mechanical competence.

3.4 Bioactivity assessment in SBF

Figure 5 shows the XRD spectra of the 25GS75RL specimens sintered at 1050°C for 1 h and then immersed in SBF for 3–28 days, together with the XRD patterns of 45S5 Bioglass® in as-sintered conditions. A significant phenomenon, in addition to the peaks of apatite phase detected in the spectra of soaked specimens, was that the crystallinity of the sintered specimens decreased with increasing immersion time in SBF. Eventually the sharp diffraction peaks of the $Na_2Ca_2Si_3O_9$ phase largely decreased after soaking in SBF for 28 days. This indicates that at least

Table 3 Apparent density, porosity and compressive strength of 45S5 Bioglass®-derived scaffolds

Material code	Apparent density (g/cm^3)	Porosity (%)	Compressive strength (MPa)
20GL80RS	1.5 ± 0.3	45.9 ± 2.2	7.2 ± 3.5
30GL70RL	1.6 ± 0.6	43.5 ± 1.7	6.8 ± 2.7
25GS75RL	1.4 ± 0.5	47.2 ± 2.7	5.4 ± 2.3

under the detection limits of XRD, the sintered 45S5 Bioglass®-derived scaffold was mainly composed of a less-crystalline $Na_2Ca_2Si_3O_9$ phase and crystalline apatite after soaking in SBF for 28 days.

Figure 6a–e illustrates typical surface morphologies of the 25GS75RL specimens sintered at 1050°C for 1 h followed by immersing in SBF for different time periods. The surfaces of the 25GS75RL scaffold appeared to have slight texture after 7 days in SBF (Fig. 6b). The surfaces undergo further topographical changes through 14 days (Fig. 6c) and 28 days (Fig. 6d). Moreover, the surfaces present after 3 and 7 days were relatively smooth compared with the globular morphology of 14 and 28 days surfaces. Following 14 days immersion, the 25GS75RL scaffold was composed of sub-micron sized globules (Fig. 6c). Furthermore, the granular apatite layer (Fig. 6e) did continue to fill the surface with increased immersion time (28 days) in SBF. Results of the EDS analysis for the surfaces of the 25GS75RL scaffolds are presented in Fig. 7a, b, measured as-sintered specimen and after 28 days of immersion in SBF. EDS analysis revealed that the surfaces of the 25GS75RL scaffolds exhibited much more concentrations of Ca and P after immersion in SBF for 28 days. As a result, the apatite formed obviously after immersion in SBF for 28 days.

In the recent work, Clupper and Hench [33–35] carried out quantitative investigations on the effect of crystallinity on the apatite formation on Bioglass® surfaces in vitro. Their findings revealed that the crystal phase $Na_2Ca_2Si_3O_9$ slightly decreased the formation kinetics of an apatite layer on the Bioglass® sample surface but it did not totally suppress the formation of such layer [33]. Moreover, it is

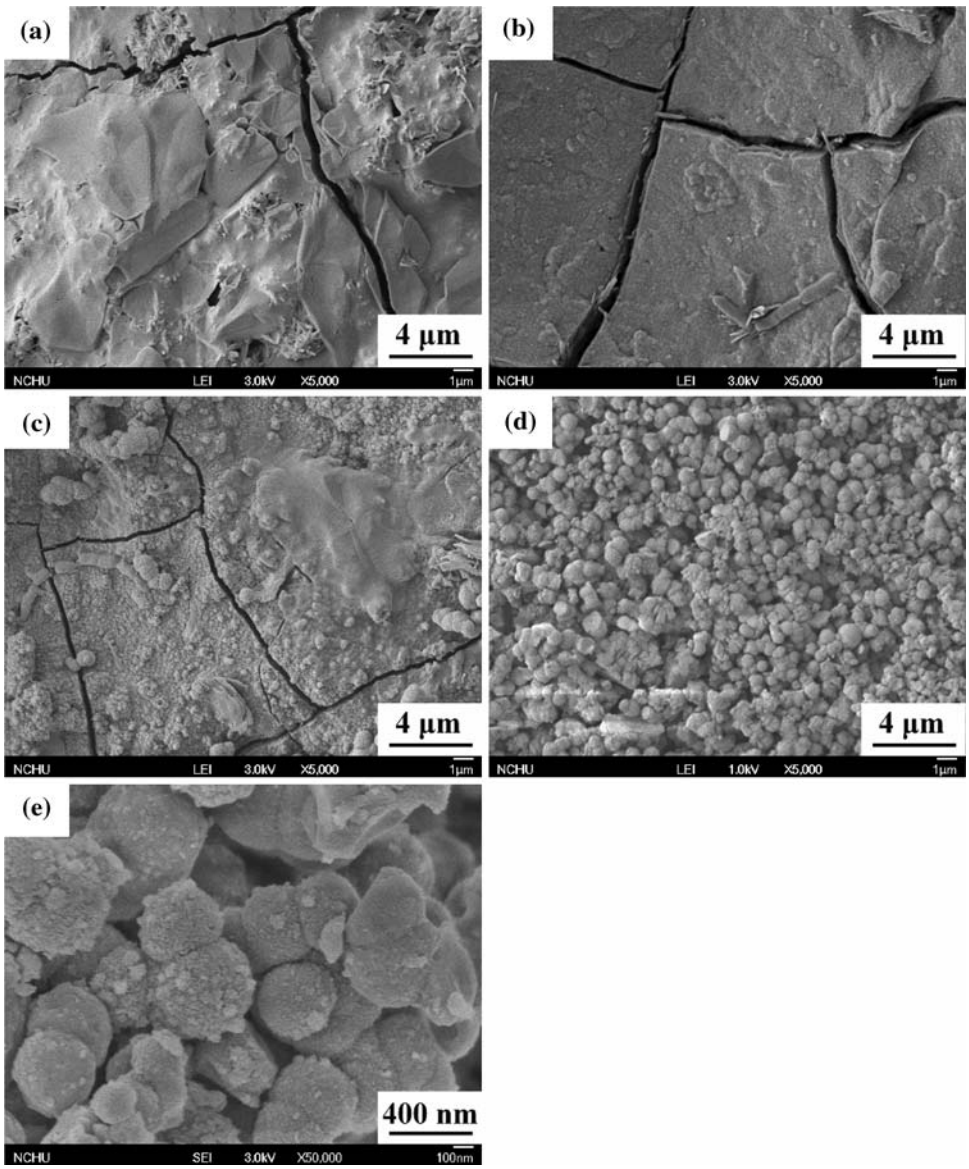

Fig. 6 Surface morphologies of 25GS75RL scaffolds sintered at 1050°C for 1 h followed by immersion in SBF for different time periods. **a** 3 days, **b** 7 days, **c** 14 days, **d** 28 days and **e** 28 days under higher magnification

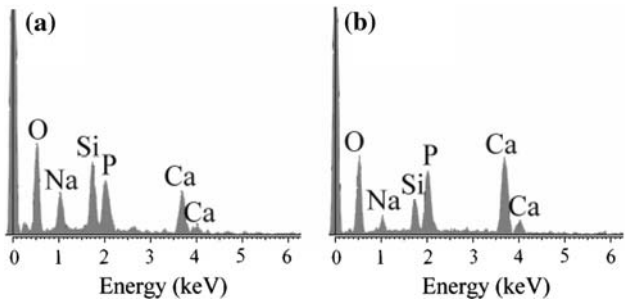

Fig. 7 EDS of 25GS75RL scaffolds: **a** as-sintered and **b** following 28 days SBF immersion

recognized that the bioreaction kinetics of a porous network can be very different from that of a dense product of the same chemical composition due to a high surface area in the foams. In addition, the bioactivity of pure $Na_2Ca_2Si_3O_9$ phase has also been reported [48]. Tissue engineering applications demand that the degradation kinetics of a scaffold should match the regeneration kinetics of new bone in vitro and/or in vivo. Chen et al. [36] stated that the high surface area in the porous network is of relevance in maintaining bioactivity and biodegradability of the sintered 45S5 Bioglass®-derived scaffolds.

After immersion in SBF for 28 days, the compressive strengths of the porous scaffolds were measured in a dry state to evaluate the effects of degradation on the mechanical properties. The compressive strengths of 20GL80RS, 30GL70RL and 25GS75RL as-sintered specimens and after immersion in SBF for 28 days are shown in Fig. 8. After the immersion test, the compressive strengths of all the scaffolds decreased. Moreover, after 28 days SBF immersion the compressive strengths of 30GL70RL and 25GS75RL scaffolds were significantly ($P < 0.05$) lower than those of 20GL80RS scaffolds.

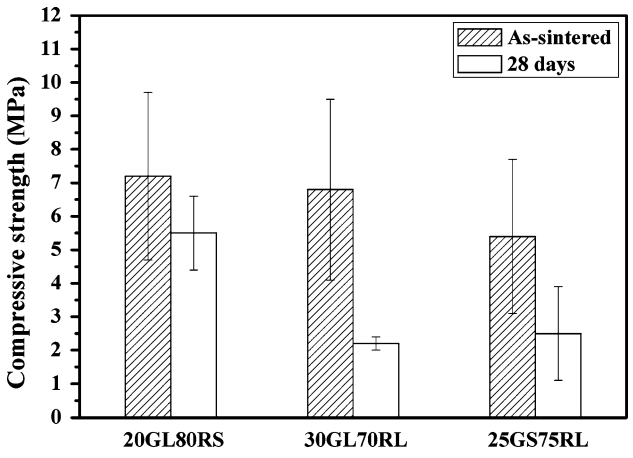

Fig. 8 Compressive strengths of 20GL80RS, 30GL70RL and 25GS75RL as-sintered specimens and following 28 days SBF immersion

4 Conclusions

In this work, glass–ceramic porous scaffolds based in the 45S5 Bioglass® have been developed. The incorporation of rice husks as the foaming agent was chosen for the elaboration of these tissue engineering constructs. According to the obtained results, the 25GS75RL specimens prepared from 45S5 Bioglass® powder (25 wt%, ≤25 μm in particle size) by forming with the rice husks (75 wt%, 355–600 μm in particle size) were found to have the highest porosity percentage and appropriate compressive strength (5.4 MPa). After immersion in SBF for 28 days, the sharp diffraction peaks of the $Na_2Ca_2Si_3O_9$ phase largely decreased and the apatite formed obviously. In this study, rice husk used as pore former was revealed to be an interesting method to fabricate porous glass–ceramic scaffolds. Furthermore, the goal of an ideal scaffold that provides sufficient mechanical support temporarily while maintaining bioactivity, and that can biodegrade at later stages is achievable with the developed 45S5 Bioglass®-derived scaffolds.

References

1. L.L. Hench, J.M. Polak, Science **295**, 1014 (2002). doi:10.1126/science.1067404
2. S.P. Bruder, in *Caplan AI in Principles of Tissue Engineering*, 2nd edn., ed. by R.P. Lanza, R. Langer, J. Vacanti (Academic Press, California, 2000), pp. 683–696
3. N. Okii, S. Nishimura, K. Kurisu, Y. Takeshima, T. Uozumi, Neur. Med. Chir. **41**(2), 100 (2001). doi:10.2176/nmc.41.100
4. T.M. Freyman, I.V. Yannas, L.J. Gibson, Prog. Mater. Sci. **46**, 273 (2001). doi:10.1016/S0079-6425(00)00018-9
5. E. Jabbarzadeh, T. Jiang, M. Deng, L.S. Nair, Y.M. Khan, C.T. Laurencin, Biotechnol. Bioeng. **98**, 1094 (2007). doi:10.1002/bit.21495
6. M.M.C.G. Silva, L.A. Cyster, J.J.A. Barry, X.B. Yang, R.O.C. Oreffo, D.M. Grant, C.A. Scotchford, S.M. Howdle, K.M. Shakesheff, F.R.A.J. Rose, Biomaterials **27**, 5909 (2006). doi:10.1016/j.biomaterials.2006.08.010
7. C. Vitale-Brovarone, E. Verné, L. Robiglio, P. Appendino, F. Bassi, G. Martinasso, G. Muzio, R. Canuto, Acta Biomater. **3**, 199 (2007). doi:10.1016/j.actbio.2006.07.012
8. H.R. Ramay, M.Q. Zhang, Biomaterials **24**, 3293 (2003). doi:10.1016/S0142-9612(03)00171-6
9. S. Sánchez-Salcedo, A. Nieto, M. Vallet-Regí, Chem. Eng. J. **137**, 62 (2008). doi:10.1016/j.cej.2007.09.011
10. D. Tadic, F. Beckmann, K. Schwarz, M. Epple, Biomaterials **25**, 3335 (2004). doi:10.1016/j.biomaterials.2003.10.007
11. M. Shin, H. Abukawa, M.J. Troulis, J.P. Vacanti, J. Biomed. Mater. Res. **84A**, 702 (2008). doi:10.1002/jbm.a.31392
12. J.M. Williams, A. Adewunmi, R.M. Schek, C.L. Flanagan, P.H. Krebsbach, S.E. Feinberg, S.J. Hollister, S. Das, Biomaterials **26**, 4817 (2005). doi:10.1016/j.biomaterials.2004.11.057
13. J. Wilson, G.H. Pigot, F.J. Schoen, L.L. Hench, J. Biomed. Mater. Res. **15**, 805 (1981). doi:10.1002/jbm.820150605
14. H. Oonishi, S. Kutrshitani, E. Yasukawa, H. Iwaki, L.L. Hench, J. Wilson, E. Tsuji, T. Sugihara, Clin. Orthop. Relat. Res. **334**, 316 (1997). doi:10.1097/00003086-199701000-00041

15. L.L. Hench, R.J. Splinter, W.C. Allen, T.K. Greenlee, J. Biomed. Mater. Res. **5**, 117 (1971). doi:10.1002/jbm.820050611
16. L.L. Hench, H.A. Paschall, J. Biomed. Mater. Res. **7**, 25 (1973). doi:10.1002/jbm.820070304
17. L.L. Hench, H.A. Paschall, J. Biomed. Mater. Res. **8**, 49 (1974). doi:10.1002/jbm.820080307
18. A.M. Gatti, G. Valdre, O.H. Andersson, Biomaterials **15**, 208 (1994). doi:10.1016/0142-9612(94)90069-8
19. A.E. Clark, L.L. Hench, J. Biomed. Mater. Res. **28**, 693 (1994). doi:10.1002/jbm.820280606
20. L.L. Hench, Curr. Opin. Solid State Mater. Sci. **2**, 604 (1997). doi:10.1016/S1359-0286(97)80053-8
21. L.L. Hench, J. Wilson, Science **226**, 630 (1984). doi:10.1126/science.6093253
22. J.R. Jones, L.L. Hench, Curr. Opin. Solid State Mater. Sci. **7**, 301 (2003). doi:10.1016/j.cossms.2003.09.012
23. A.R. Boccaccini, J. Mater. Sci. Mater. Med. **14**, 350 (2003). doi:10.1023/A:1023266902662
24. K. Ohura, T. Nakamura, T. Yamamuro, Y. Ebisawa, T. Kokubo, Y. Kotoura, M. Oka, J. Mater. Sci. Mater. Med. **3**, 95 (1992). doi:10.1007/BF00705275
25. J.E. Davies, N. Baldan, J. Biomed. Mater. Res. **36**, 429 (1997). doi:10.1002/(SICI)1097-4636(19970915)36:4<429::AID-JBM1>3.0.CO;2-G
26. Q.Z. Chen, K. Rezwan, V. Françon, D. Armitage, S.N. Nazhat, F.H. Jones, A.R. Boccaccini, Acta Biomater. **3**, 551 (2007). doi:10.1016/j.actbio.2007.01.008
27. J.R. Jones, L.L. Hench, J. Biomed. Mater. Res. **68B**, 36 (2004). doi:10.1002/jbm.b.10071
28. A.R. Boccaccini, Q.Z. Chen, L. Lefebvre, L. Gremillard, J. Chevalier, Farad. Dis. **136**, 27 (2007). doi:10.1039/b616539g
29. L.L. Hench, J. Am. Ceram. Soc. **81**(7), 1705 (1998)
30. N.K. Sharma, W.S. Williams, A. Zangvil, J. Am. Ceram. Soc. **67**, 715 (1984). doi:10.1111/j.1151-2916.1984.tb19507.x
31. S. Chandrasekhar, K.G. Satyanarayana, P.N. Pramada, P. Raghavan, T.N. Gupta, J. Mater. Sci. **38**, 3159 (2003). doi:10.1023/A:1025157114800
32. P. Li, C. Ohtsuki, T. Kokubo, K. Nakanishi, N. Soga, N. Nakamura, T. Yamamuro, J. Mater. Sci. Mater. Med. **4**, 127 (1993). doi:10.1007/BF00120381
33. O.P. Filho, G.P. LaTorre, L.L. Hench, J. Biomed. Mater. Res. **30**, 509 (1996). doi:10.1002/(SICI)1097-4636(199604)30:4<509::AID-JBM9>3.0.CO;2-T
34. D.C. Clupper, J.J. Mecholsky Jr, G.P. LaTorre, D.C. Greenspan, J. Biomed. Mater. Res. **57**, 532 (2001). doi:10.1002/1097-4636(20011215)57:4<532::AID-JBM1199>3.0.CO;2-3
35. D.C. Clupper, J.J. Mecholsky Jr, G.P. LaTorre, D.C. Greenspan, Biomaterials **23**, 2599 (2002). doi:10.1016/S0142-9612(01)00398-2
36. Q.Z. Chen, I.D. Thompson, A.R. Boccaccini, Biomaterials **27**, 2414 (2006). doi:10.1016/j.biomaterials.2005.11.025
37. D.C. Clupper, L.L. Hench, J. Non-Crys, Solid **318**, 43 (2003)
38. G. Daculsi, R.Z. LeGeros, M. Heughebaert, Calcif. Tissue Int. **46**, 20 (1990). doi:10.1007/BF02555820
39. T. Lin, C. Su, C. Chang, J. Biomed. Mater. Res. **36**, 91 (1997). doi:10.1002/(SICI)1097-4636(199707)36:1<91::AID-JBM11>3.0.CO;2-M
40. N. Kawai, S. Niwa, M. Sato, Y. Sato, Y. Suwa, I. Ichihara, J. Biomed. Mater. Res. **37**, 1 (1997). doi:10.1002/(SICI)1097-4636(199710)37:1<1::AID-JBM1>3.0.CO;2-W
41. J.D. Currey, Clin. Orthop. Relat. Res. **73**, 210 (1970). doi:10.1097/00003086-197011000-00023
42. K.A. Hing, S.M. Best, W. Bonfield, J. Mater. Sci. Mater. Med. **10**, 135 (1999). doi:10.1023/A:1008929305897
43. J.R. Jones, L.M. Ehrenfried, L.L. Hench, Biomaterials **27**, 964 (2006). doi:10.1016/j.biomaterials.2005.07.017
44. L.J. Gibson, M.F. Ashby, *Cellular Solids: Structure and Properties*, 2nd edn (Pergamon, Oxford, 1999), pp. 117–118, 209–212
45. C.H. Turner, in *Burr DB in Bone Mechanics*, ed. by S.C. Cowin (CRC Press, Boca Raton, 1989), pp. 1–11
46. N. Tamai, A. Myoui, T. Tomita, T. Nakase, J. Tanaka, T. Ochi, J. Biomed. Mater. Res. **59**, 110 (2002). doi:10.1002/jbm.1222
47. D.R. Carter, W.C. Hayes, Science **194**, 1174 (1976). doi:10.1126/science.996549
48. O. Peitl, E.D. Zanotto, L.L. Hench, J. Non-Crys, Solid **292**, 115 (2001)